

# STRUCTURE-PROPERTY CORRELATION OF LRS (GRADE-B) STEEL WELDMENT

\* B.K. MONDAL, \*\* J. MAITY

\* M.Tech student of Foundry & Forge Technology; \*\*Lecturer, Department of Materials & Metallurgical Engineering, National Institute of Foundry & Forge Technology, Hatia, Ranchi-834003.

## ABSTRACT

LRS (Grade-B) steel, a structural material used in ship hull, was MIG welded in Argo-shield atmosphere. Microstructure & hardness variations were studied across the weldment. Tensile properties and tensile-failed surfaces of parent steel and weld were also investigated. Structure of the weldment was correlated with its property and a comparison was made with the property of parent steel to ascertain the effectiveness of MIG welding. Considerable hardness & microstructural variation was found across the weldment. Weld hardness & tensile strength were found higher than that of parent steel indicating an expected satisfactory fatigue performance of weld in service.

## Keywords

LRS (Grade-B steel), MIG welding, weldment, macrostructure, microstructure, hardness variation, tensile properties, fractography.

## 1. INTRODUCTION

The material used in ship hull or tanker hull is usually the carbon-manganese steel of different grades. Major joining process in construction of ship is welding. The construction process is based on the requirements laid down by regulatory agencies viz. Lloyds Register of Shipping(LRS), American Bureau of Shipping (ABS) etc. Gas shielded flux cored arc welding and electrogas welding with 99% CO<sub>2</sub> gas of carbon-manganese steel result in a stronger weld with a wide variation of microstructure and property across the weldment [1]. Weld property strongly depends on the nature of

phase transformation guided by heat input, alloying addition through electrode and cooling characteristic for the welding process used. Various factors acting together complicate the transformation feature leading to morphologically complex microstructure[2]. This paper investigates the effectiveness of MIG welding with Argo-shield gas on LRS(Grade-B) steel, a ship hull material, through structure- property correlation across the weldment in comparison with the parent steel.

## 2. EXPERIMENTAL

### 2.1 Test Material

The material used in this study was LRS(Grade- B) steel provided by Garden Reach Shipbuilders & Engineers Ltd., Kolkata, India. Chemical composition of this steel is presented in Table 1.

### 2.2 MIG Welding

Butt joint welds were produced with steel plates of 8 mm. thickness in automatic MIG welding machine (KEMPPI, PRO MIG-530) using ER70S-6 electrode(solid wire) along with Argo-shield gas (95%Ar+5%CO<sub>2</sub>) at a gas flow rate 20 lt/min. Chemical composition of electrode wire is given in Table 2. Single V groove joint was welded with three passes in a sequence -root pass, second pass, back gouging followed by third (final) pass. Details of welding parameters are present in Table 3.

### 2.3 Metallography

#### 2.3.1 Study of Macrostructure

A cross section was cut across the weldment perpendicular to welding direction and was macroetched

by (4% HNO<sub>3</sub> + 96% Methanol) solution to reveal the macrostructure of weld metal & HAZ. Photograph of this macrostructure was taken at 10X.

### 2.3.2 Study of Microstructure

Microstructures of as received steel (parent steel) and that at different points across the weldment were studied under metallurgical microscope (OLYMPUS, CK40M-F200). Etchant used was 2% NITAL (2% HNO<sub>3</sub> + 98% Methanol). Accordingly photomicrographs of parent steel & welded plate were taken. For welded plate at different sites on the cut out cross section photomicrographs were taken across the weldment along a line lying at 2.5 mm above the bottom edge of the plate.

Quantitative metallography was also carried out on the microstructures studied across the weldment. Point count method was used to determine percentage of different phases present. ASTM grain size number of the microstructures having grain boundary clarity was also determined by Jefferies Planimetric method [3].

### 2.4 Hardness Test

Hardness of parent steel and that across the weldment (along the line considered for metallographic study) were measured with 30 kg load in Vickers hardness tester (LEIPZIG, HPO 250).

### 2.5 Tensile Test

Unnotched round cylindrical tensile specimen, at first, was machined out from the welded plate keeping weldment at the middle of gauge. However, during tensile test this specimen failed along a cross-section lying outside the weldment. Therefore, in order to cause failure through the weldment, single edge notched (SEN) flat specimens (Fig.1) were chosen for tensile test of parent steel and weld. For weld, SEN specimen was machined out from the welded plate keeping notch tip at weld-centerline. Tensile test on SEN flat specimens of parent metal and weld was carried out in universal testing machine (INSTRON-8501) at a strain rate 10<sup>-3</sup> s<sup>-1</sup>.

## 3. Results & Discussion

Macrostructure of weldment, hardness variation across weldment and sites of microstructural study (A, B, C, D, E & F) are shown in Fig.2. Microstructures of parent steel and welded plate (across the weldment with respect to sites mentioned in Fig.2) are shown in Fig.3 & 4. Quantitative metallography and hardness data are presented in Table 4. Results of tensile test are presented in Table 5. Photomicrographs (Fig.3 & 4) of all the microstructures reveal the presence of ferrite and pearlite. Parent steel, Base metal and HAZ have a conventional ferrite-pearlitic microstructure with varying grain size, mainly depending on the cooling rate. Although weld metal also contains ferrite & pearlite, it is more enriched with pearlite than the parent steel/base metal. Most importantly, ferrite phase present in weld microstructure has different morphology. Weld microstructures (site D, E, & F) are compared with those published by other researchers [4-7] and accordingly, polygonal ferrite (PF) or grain boundary ferrite (GBF), ferrite side plate (FSP) & acicular ferrite (AF) are identified. Ferrite formation temperature falls in the following order: PF(GBF) –FSP-AF [4]. PF is basically the proeutectoid ferrite which forms while cooling below the Ac<sub>3</sub> temperature at prior austenite grain boundary having usually a polygonal shape. When temperature further falls down, with increased degree of undercooling there is a tendency for ferrite to grow bilaterally from the prior austenite grain boundaries in the form of plates, called ferrite side plates (FSP). At still lower temperature (more undercooling) austenite transforms into fine irregular needle like structures, generally referred to as acicular ferrite. Acicular ferrite is highly substructured non-equiaxed ferrite that forms by a mixed diffusion and shear mode of transformation.

The weld undergoes considerable alloying (Mn) addition through welding electrode. Presence of alloying element (Mn) causes solid solution strengthening and shifts the eutectoid point to left [8] resulting in higher percentage of pearlite in weld microstructure. As a result weld has higher hardness and strength than the

parent steel. Apart from this, presence of acicular ferrite also contributes to the higher strength of weld [4]. MIG welding in the present study, results in a strength improvement of the hull material equivalent to that reported for gas shielded flux cored arc welding and electrogas welding of carbon-manganese steel using 99% CO<sub>2</sub> [1]. Across the weldment, from weld centerline to HAZ, hardness value gradually falls down due to more dilution of base metal causing less alloying addition. The part of HAZ nearer to base metal (site-B) has finer structure (more ASTM grain size number) and more pearlite content than the other parts of HAZ. This is the result of faster cooling rate of the HAZ portion nearer to base metal. Faster cooling rate shifts the eutectoid point to left resulting in more percentage pearlite in microstructure and brings down the eutectoid transformation temperature to provide finer structure [9]. Thus from weld metal-HAZ interface to HAZ-base metal interface hardness gradually increases and then goes down to approach the base metal hardness at the end of HAZ. Thereafter, hardness remains almost unchanged within unaffected base metal.

SEM fractographs (Fig.5) reveal dimple rupture through microvoid coalescence both in parent steel and weld. However, weld-fracture surface exhibits shallow & smaller dimples in contrast with deep & large dimples of the fracture surface of parent steel. This is in agreement with the higher hardness and strength of weld than that of parent steel.

The LRS (grade- B) steel, when used in ship hull, experiences fatigue loading in sea water. Endurance limit of carbon steel usually comes around 50% of ultimate tensile strength [10,11]. Therefore, weld with higher ultimate tensile strength than the parent steel is expected to provide satisfactory fatigue resistance representing the success of MIG welding.

#### 4. Conclusions

- MIG welding of LRS Grade-B steel with Argo-shield gas and ER70S-6 electrode generates more pearlite enriched stronger & harder weld. The strength improvement is equivalent to that reported for gas shielded flux cored arc welding and electrogas welding processes using 99% CO<sub>2</sub>.
- Considerable hardness & microstructural variation is observed across the weldment.
- Weld microstructure reveals typical ferrite-morphology viz. acicular, side plate and polygonal.
- Weld is expected to perform satisfactorily under fatigue loading.

#### References

- Jack Still & Juban Speck: "Weld Metal And Heat Affected Zone (HAZ) Properties of Tanker Hull Structures", Indian Welding Journal, January 2003,36(1), pp.23-27.
- G. den Ouden, J.G. Verhagen and G.W. Tichelaar: "Influence of Chemical Composition on Mild Steel Weld Metal Notch Toughness", Welding Journal (Welding Research Supplement), March 1975,54(3), pp.87s-94s.
- Xiwen xie: "Metallurgical property testing" in Steel Heat treatment Hand Book, 1st ed., George E. Totten and Maurice A.H. Howes, ed., Marcel Dekker, Inc, New York, NY, 1997, p.995.
- Y. Komizo and Y. Fukada, "Toughness improvement in weld metal of carbon and HSLA steels in Japan" in Advances in Welding Metallurgy, Proceedings from the First United States- Japan Symposium, American Welding Society, Japan Welding Society & The Japan Welding Engineering Society, San Francisco, California, Yokohama, Japan, 1990, pp.227-250.
- J.M.B Losz and K.D Challenger, "HAZ Microstructures in HSLA Steel Weldments" in Advances in Welding Metallurgy, Proceedings from the First United States- Japan Symposium, American Welding Society, Japan Welding Society & The Japan Welding Engineering Society, San Francisco, California, Yokohama, Japan, 1990, pp.207-226.
- Stephen A. Court, and Geoffrey Pollard : "The Development of Microstructure in C-Mn Steel Weld Deposits" in Welding metallurgy of structural steels, J.Y. Koo, ed., Metallurgical Society, Warrendale, Pennsylvania, 1987, pp.505-516.
- C. Thaulow, A.J. Paauw, and G.Rorvik : "Fracture Mechanics Testing of Weld metal for Low carbon Microalloyed steel" in Welding metallurgy of structural steels, J.Y. Koo, ed., Metallurgical Society, Warrendale, Pennsylvania, 1987, pp.277-301.
- R. A. Higgins, "The properties of Engineering Material", 2nd ed., Edward Arnold, 338 Euston Road, London, 1994, p.233.
- T.V. Rajan, C.P. Sharma, Ashok Sharma: "Heat Treatment- Principles and Techniques". Revised ed., Prentice-Hall of India Pvt. Ltd., New Delhi, 1994, pp.79-80.
- Joseph B.Conway and Lars H. Sjobahl: "Analysis and Representation of Fatigue Data", ASM International, Materials Park, Ohio, 1991, p.34.
- Eliahu Zahavi : "Fatigue Design Life Expectancy of Machine Parts", CRC Press, Boca Raton, Florida, 1996, p.54.

**Table 1: Chemical Composition of LRS (Grade-B) Steel.**

C (Wt%)	Mn (Wt%)	S i(Wt%)	P (Wt%)	S (Wt%)
0.21	0.8	0.35	0.035	0.035

**Table 2: Chemical Composition of Welding Electrode.**

C (Wt%)	S i(Wt%)	Mn (Wt%)	S (Wt%)	P (Wt%)	Cu (Wt%)
0.1	0.9	1.6	0.02	0.02	0.2

**Table 3: Welding Parameters.**

Bead layers	Current (Amps)	Voltage (Volt)	Wire feed rate (m/min)	Travel speed (cm/min)	Heat input (KJ/cm)
Root pass	195	20.1	4.7	21.15	11.12
Second pass	270	24.4	7.4	37.6	10.51
Third pass	253	25.5	8.2	37.5	10.32

**Table 4: Quantitative Metallography & Hardness Data.**

Specimen	% Ferrite	%Pearlite	ASTM Grain Size No.	Hardness (HV)	
Parent steel	89.6	10.4	12.04	148	
Welded steel	Site A (Base metal)	89.99	10.1	12.07	143
	Site B (HAZ)	76	24	12.69	159
	Site C (HAZ)	82	18	12.25	158.5
	Site D (Weld metal, fusion zone)	21.75	78.25	-	189
	Site E (Weld center)	23	77	-	193.5
	Site F (HAZ- weld metal interface)	56	44	-	156

**Table 5: Results of Tensile Test**

Specimen	0.2% Proof stress (MPa)	Ultimate tensile strength (MPa)	% Elongation	% Area reduction
Parent steel	452.7	531	17.41	30.48
Weld	528.3	652	11.21	21.3



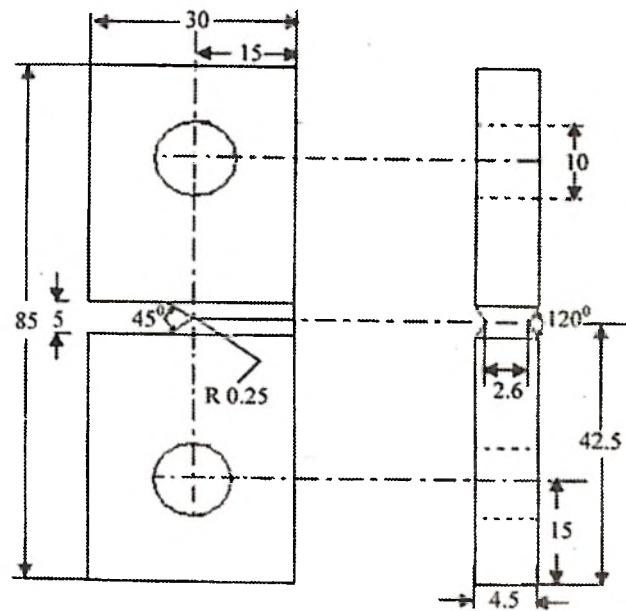


Fig.1: Single edge notched tensile specimen.  
(All dimensions are in mm.)

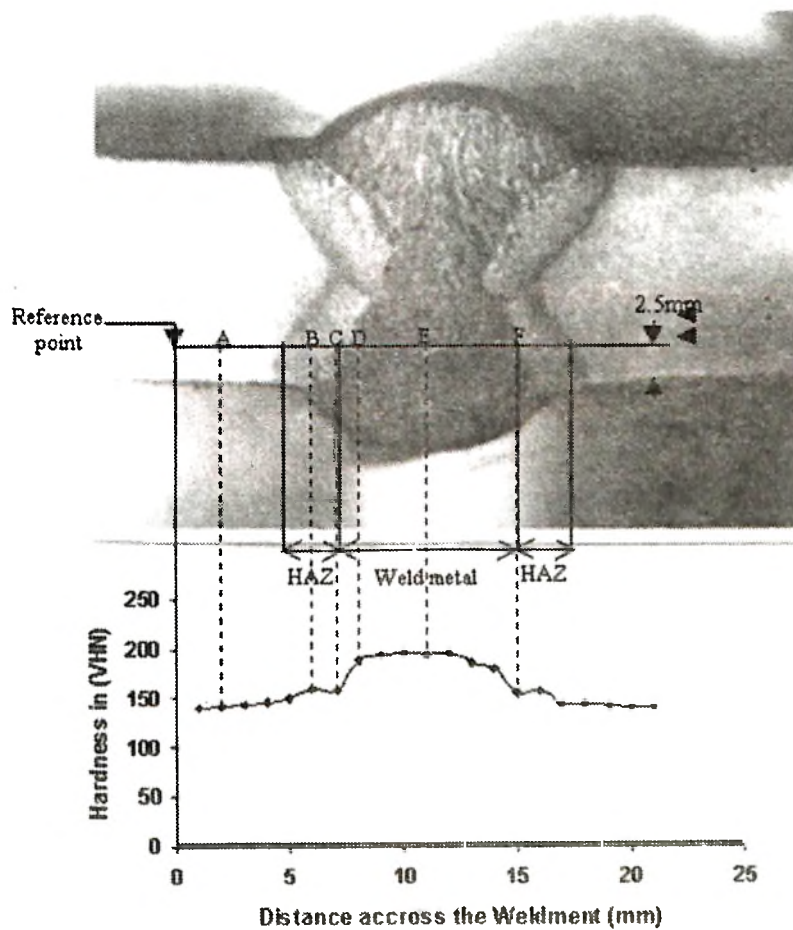


Fig.2: Macrostructure of weldment, hardness variation across weldment and sites of microstructural study (A, B, C, D, E, F).

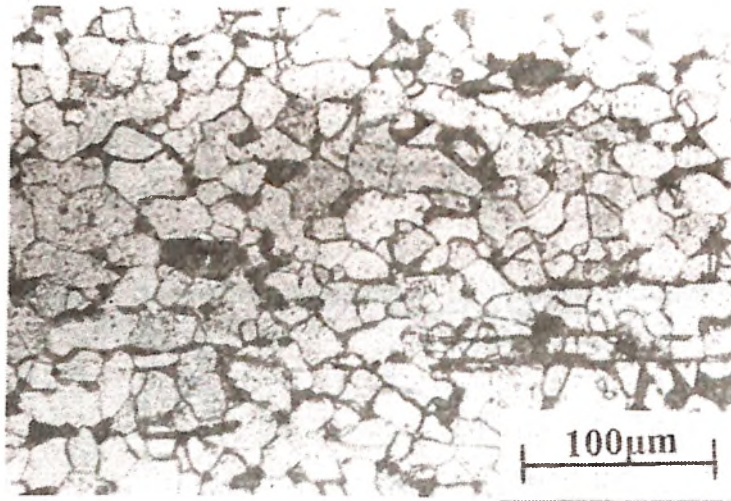


Fig.3. Microstructure of parent steel.

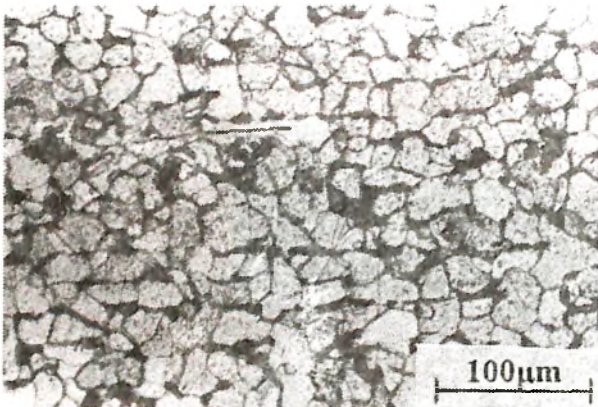


Fig.4(a) Site A: Base metal consisting of ferrite (bright) and pearlite (dark).

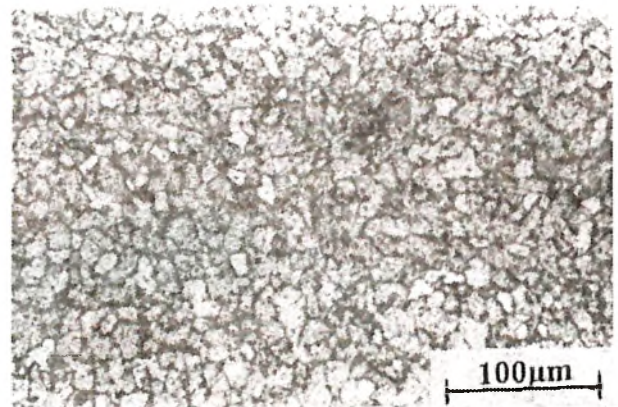


Fig.4(b) Site B: Heat Affected Zone (HAZ) near base metal containing ferrite (bright) and pearlite (dark) with much finer structure than site A.

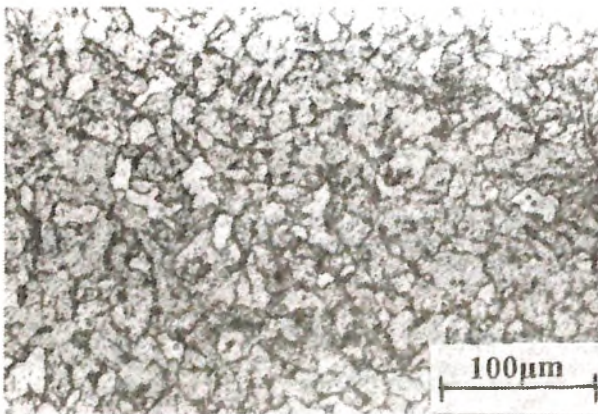


Fig.4(c) Site C: HAZ near weld metal containing ferrite + pearlite with relatively coarser structure than site B.

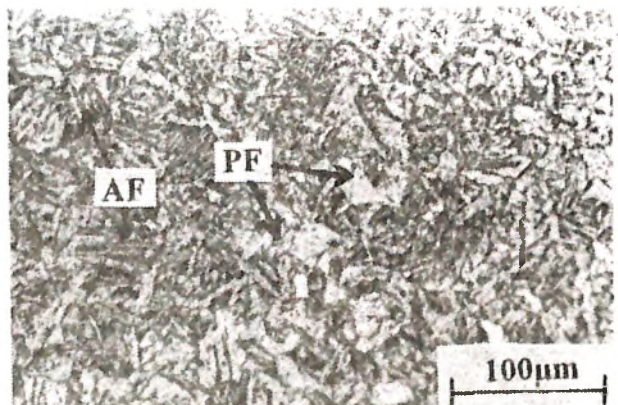


Fig.4(d) Site D: Fusion zone containing PF & AF along with pearlite.



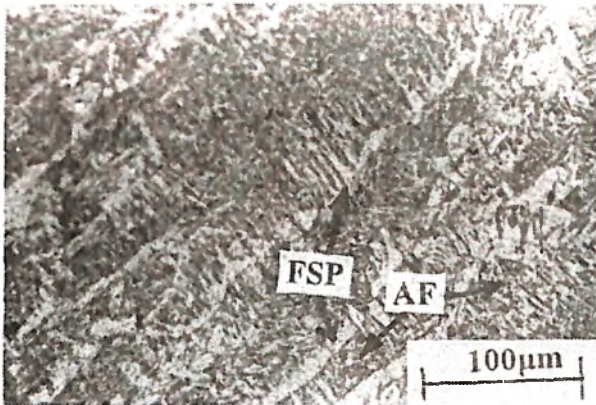


Fig.4(e) Site E: Weld metal at weld centerline showing mostly FSP and AF along with pearlite.

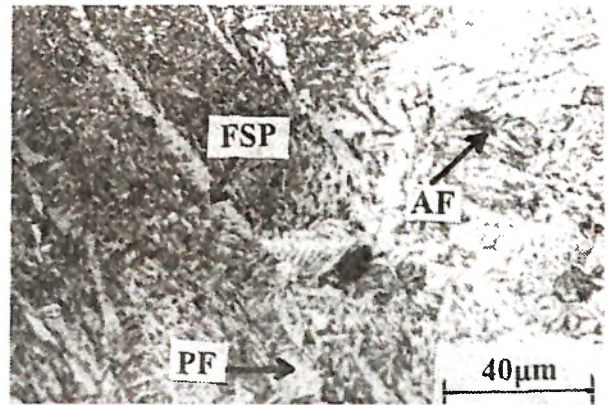


Fig.4(f) Site F: HAZ-Weld metal interface showing the transition between pearlite enriched (darker) weld metal & ferrite enriched(brighter) HAZ. A cluster of PF, AF along with FSP is visible on HAZ side.

Fig.4: Microstructures across the weldment (PF-polygonal ferrite,FSP-ferrite side plate, AF-acicular Ferrite)

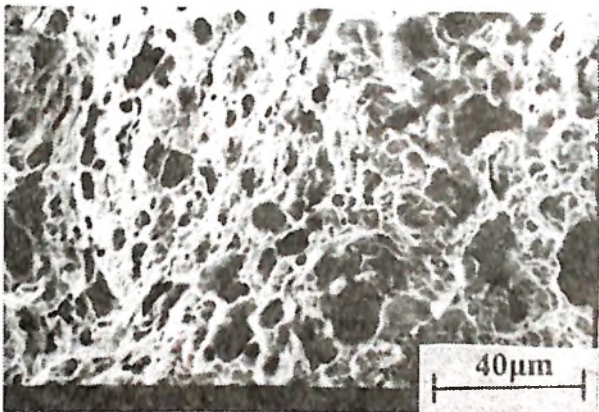


Fig.5(a) Fracture surface of parent steel (deep & large dimples).

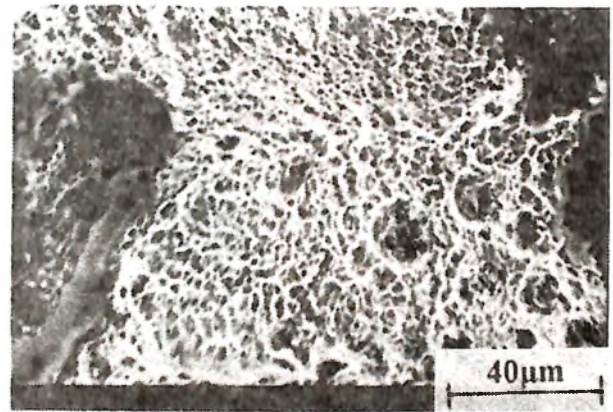


Fig.5(b) Fracture surface of weld (shallow & smaller dimples).

Fig.5: SEM Fractograph of tensile tested specimens.

List of Tables

- Table 1: Chemical Composition of LRS (Grade-B) Steel.
- Table 2: Chemical Composition of Welding Electrode.
- Table 3: Welding Parameters.
- Table 4: Quantitative Metallography & Hardness Data.
- Table 5: Results of Tensile Test.

List of Figures

- Fig.1: Single edge notched tensile specimen.
- Fig.2: Macrostructure of weldment, hardness variation across weldment and sites of microstructural study (A, B, C, D, E, F).
- Fig.3: Microstructure of parent steel.
- Fig.4: Microstructures across the weldment (PF-polygonal ferrite,FSP-ferrite side plate, AF-acicular Ferrite)
  - Fig.4(a) Site A: Base metal consisting of ferrite (bright) and pearlite (dark).

- Fig.4(b) Site B: Heat Affected Zone (HAZ) near base metal containing ferrite (bright) and pearlite (dark) with much finer structure than site A.
- Fig.4(c) Site C: HAZ near weld metal containing ferrite + pearlite with relatively coarser structure than site B.
- Fig.4(d) Site D: Fusion zone containing PF & AF along with pearlite.
- Fig.4(e) Site E: Weld metal at weld centerline showing mostly FSP and AF along with pearlite.
- Fig.4(f) Site F: HAZ-Weld metal interface showing the transition between pearlite enriched (darker) weld metal & ferrite enriched(brighter) HAZ. A cluster of PF, AF along with FSP is visible on HAZ side.

Fig.5: SEM Fractograph of tensile tested specimens.

- Fig.5(a) : Fracture surface of parent steel (deep & large dimples).
- Fig.5(b) : Fracture surface of weld (shallow & smaller dimples).